

## Comparative Experimental Performance Study of Four Fixed Photovoltaic Subfields Under Saharan Climate: A Case Study in Oued-Nechou, Ghardaïa

Bouramdane Abderraouf<sup>1\*</sup>, Louazene Mohammed Lakhdar<sup>2</sup> and Benmir Abdelkader<sup>3</sup>

Submitted: 10/02/2024 Revised: 15/05/2024 Accepted: 22/05/2024

**Abstract:** An experimental study at a 1.1 MWp photovoltaic plant in Oued-Nechou, Ghardaïa, evaluated the performance of four fixed 100 kWp subfields using crystalline silicon (mc-Si, pc-Si) and thin-film (a-Si, CdTe) technologies. Data were collected over four days, each representing a different season, to assess peak output, total power generation, and long-term performance under various meteorological conditions. The a-Si subfield exhibited the highest overall power output during the study, with a peak of 99.98 kW on May 1st, nearing its optimal capacity and marking the highest output in 2016. On the same day, peak outputs for the other subfields were recorded as follows: CdTe at 96.67 kW, mc-Si at 95.67 kW, and pc-Si at 84.06 kW. Over four days, the daily average power output from sunrise to sunset revealed that the mc-Si subfield had the highest average output at 47.06 kW, while the pc-Si subfield recorded a lower average of 39.46 kW.

Furthermore, performance evaluation based on augmentation percentages for mean output power revealed that the amorphous silicon (a-Si) subfield consistently outperformed the other technologies. On July 1st, the a-Si subfield recorded a significant power gain of 19.250% compared to the polycrystalline silicon (pc-Si) subfield. On October 1st, it showed a similar gain of 19.206% over the pc-Si subfield. Moreover, Real-time data, collected at four-minute intervals, was used to assess the impact of key meteorological parameters such as solar irradiance, modeled irradiance, ambient and module temperatures, wind speed, and relative humidity on the daily power output of photovoltaic subfields. The analysis revealed a strong positive correlation between power generation, sunshine duration, and light intensity. Longer hours of sunshine and higher light intensity were found to enhance power output.

**Keywords :** Production Photovoltaic, Comparative Study, Experimental Simulation, Fixed Subfields, Output Power, Real Time Measurement, Power Augmentation, Meteorological data.

### Introduction

The increasing need for energy and global environmental concerns, along with the continuous advancements in renewable energy technologies, are creating new avenues for the usage of renewable energy resources. One of the best methods for utilizing solar energy is through photovoltaic

technology. The most plentiful, limitless, and pure renewable energy source available today is solar energy, with the amount of solar electricity that the world receives being around  $1.8 \times 10^{11}$  MW, a far greater amount than the current rate of all energy consumption. A variety of research, such as Singh [1]. Looked at the relationship between location and the power output of different solar module technologies. The energy performance of multiple module technologies was examined by Carr and Pryor [2]. And Del Cueto [3]. In Perth, Australia, and the NREL laboratory, respectively. These studies confirm that summertime is the best time for thin-film technology to operate. Additionally, Cristina Cañete [4]. Investigated the energy performance of four distinct photovoltaic module technologies over the course of a year in Southern Spain's meteorological conditions. The study concluded that during the summer, a-Si and a-Si/mc-Si modules excelled, while CdTe and pc-Si modules

*1Laboratory of Electrical Engineering (LAGE),  
Department of Electrical Engineering, University of  
kasdi Merbah Ouargla, Ouargla 30000, Algeria*

*2 Department of Electrical Engineering, kasdi  
Merbah Ouargla University, Ouargla, OU 30000  
ALGERIA*

*3Electrical Engineering Department, University of  
kasdi Merbah Ouargla, Ouargla, OU 30000  
ALGERIA*

*Corresponding author: Bouramdane. Abderraouf (e-  
mail: bouramdane.abderraouf@univ-ouargla.dz).*

performed better in winter. S. Edalati [5]. Also looked into the performance comparison of two grid connected photovoltaic technologies, mono and polycrystalline, in a dry climate. Kamal Attari [6]. Studied the assessment of two grid connected photovoltaic systems in two separate locations: one combination system, with 5.4 kWp put on the faculty roof of Tetouan, and the other, with 5 kWp positioned on the roof of a commercial building in Tangier. Where M. Effendy Ya'acob [7]. Who examined three different PV system types at a particular Malaysian location, evaluated them based on their ability to generate energy and their real performance. Wherever it was discovered the tracking flat (TF) system is therefore determined to be appropriate for use as future grid-connected PV generators in tropical climate regions. Photovoltaic (PV) technology has garnered attention locally in recent years due to the increasing global demand for energy, especially in African countries, primarily in Ghardaïa state, Algeria. This is mostly due to how easy it is to use PV technology. The primary goal of this research is to evaluate and compare the performance of four photovoltaic subfields installed at the OUED-NECHOU photovoltaic center: amorphous silicon (a-Si), cadmium telluride (CdTe), monocrystalline silicon (mc-Si), and polycrystalline silicon (pc-Si), all positioned at a 30° tilt angle. This in-depth study aims to assess the effectiveness of each technology by examining key metrics such as maximum output power (kWp) and daily power generation

.Additionally, the analysis focuses on tracking daily performance to identify the subfield demonstrating superior efficiency. The augmentation percentage, based on daily mean output power (kW), is

employed to determine which subfield serves as the benchmark in power production, highlighting the one that consistently exhibits a power gain compared to the others during the evaluation period. To further evaluate performance, this study evaluates the significant influence of environmental factors on the performance of photovoltaic subfields, specifically assessing the impact of key meteorological conditions solar irradiance ( $W/m^2$ ) at a 30° tilt, PV model irradiance ( $W/m^2$ ), ambient temperature ( $^{\circ}C$ ), module temperature ( $^{\circ}C$ ), wind speed (m/s), and relative humidity (%). Additionally, the study explains the variations in power production observed across the different measured days.

## II. Geographic Data Of The Photovoltaic Power Plant Center At Sktm Oued-Nechou, Ghardaïa

The power plant facility, built by the Algerian Electricity Production Company (SPE), is located approximately 15 km north of Ghardaïa city, near the village of OUED-NECHOU. It has a production capacity of 1.1 MWp and is situated at a latitude of 32°24'N and a longitude of 3°48'E, with an altitude of 566 meters. Completed within a 12-month timeframe, the photovoltaic power plant spans a land area of 10 hectares, bordered to the north and west by National Road (N°01) and to the south and east by an empty plot. The OUED-NECHOU region is known for its high solar radiation, peaking between 900  $W/m^2$  and 1000  $W/m^2$  during the summer. It experiences a dry Saharan climate characterized by extreme temperatures, intense solar radiation, and frequent sandstorms typical conditions for the southern regions.



**Fig. 1. Geographical location of the photovoltaic power plants 1.1MWp OUED-NECHOU, Ghardaïa City.**

### III. Description Of The Photovoltaic Installation 1.1Mwp At Oued-Nechou, Ghardaïa

The power station at OUED NECHOU in Ghardaïa was recently upgraded with a photovoltaic installation that is grid-connected, boasting a peak power capacity of 1.1 MWp. The installation is oriented directly towards the south, with the solar panels inclined at an angle of 30°.

The photovoltaic station comprises eight subfields, including four fixed subfields that incorporate different technologies such as cadmium telluride (CdTe), amorphous silicon (a-Si), polycrystalline silicon (pc-Si), and monocrystalline silicon (mc-Si). Each subfield consists of a series-connected array of photovoltaic modules connected in series with a capacity close to 100 kW. This setup is specifically designed to evaluate the effectiveness of

these PV technologies under the southern climate conditions, as shown in the technical parameters presented below.

- c) Sub-field (3) has a capacity of 108 kWp with a fixed thin-film structure using Cadmium Telluride (CdTe), and the peak power output of the PV panel is 80 Wp.
- d)-Sub-field (4): has a capacity of 100,116 kWp with a fixed amorphous silicon structure (a-Si), and the peak power output of the PV panel is 103 Wp.
- e)- Sub-field (5): has a capacity of 105 kWp with a fixed monocrystalline silicon structure (mc-Si), and the peak power output of the PV panel is 250 Wp.
- f)- Sub-field (6): has a capacity of 98.7 kWp with a fixed polycrystalline silicon structure (pc-Si), and the peak power output of the PV panel is 235 Wp

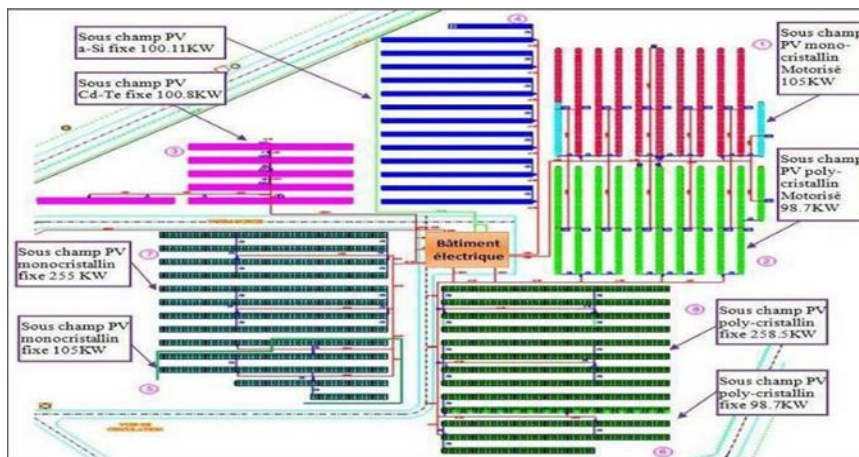


Fig. 2. Distribution of Subfields in OUED-NECHOU Photovoltaic Center, Ghardaïa City .

The fixed photovoltaic technologies associated with each PV subfield used in the comparative study

presented in this research paper are illustrated in Fig 3.



Fig. 3. Distribution The four fixed photovoltaic technologies mc-Si, and pc- Si , a-Si, CdTe used in comparsion

To gain a comprehensive understanding of this study, it is essential to grasp the electrical properties

of a range of photovoltaic technologies, including a-Si, Cd-Te, mc-Si, and pc-Si, as outlined in Table I.

**TABLE I.** Main Technical Characteristics of Photovoltaic Technologies

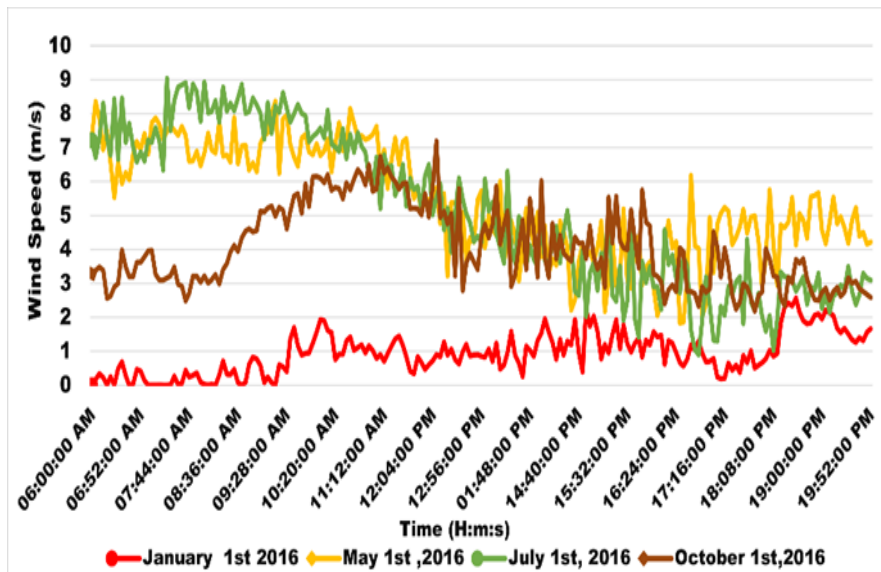
PV Subfields	<i>mc-Si</i>	<i>Pc-Si</i>	<i>a-Si</i>	<i>CdTe</i>
Peak power	250 Wc	235 Wc	103 Wc	80 Wc
Module performance	15.35%	14.43%	7.1%	11.1 %
Max voltage (V <sub>mpp</sub> )	30,35 V	29,04 V	30,4 V	48,5 V
Max intensity(I <sub>mpp</sub> )	8,24 A	8,10 A	3,39 A	1,65 A
Surface (m <sup>2</sup> )	1.63	1.63	1.45	0.72
Open circuit voltage (V <sub>oc</sub> )	37,62 V	36,94 V	41,1 V	60,8 V
NOCT	7 +/- 2 [°C]	7 +/- 2 [°C]	49 [°C]	45 [°C]
Temperature coefficient (I <sub>sc</sub> )	0,03% [°C]	0,04% [°C]	0,08% [°C]	0,04% [°C]
Temperature coefficient (V <sub>oc</sub> )	- 0,34% [°C]	- 0,32% [°C]	-0,33% [°K]	-0,20% [°K]
Temperature coefficient (P <sub>max</sub> )	-0,43% [°K]	-43% [°C]	-0,20% [°K]	-0,25% [°K]
Wight	21,5 kg	21,5 kg	20,8 kg	12 kg
Dimensions	1645 x 990 x 40 mm	1645 x 990 x 40 mm	1308 x 1108x 35 mm	1200x 600x6,8 mm

#### IV. Climatic Conditions

IV.1. Wind Speed (W/m<sup>2</sup>) and Relative Humidity (%) Accurate weather data is essential for evaluating the impact of meteorological factors on the performance of photovoltaic technologies. This study utilized a data acquisition system located on the rooftop of the Technical Room at the photovoltaic power plant, equipped with calibrated sensors to measure key climatic parameters. These parameters include solar irradiance (W/m<sup>2</sup>) at a 30° tilt, ambient temperature (°C), module temperature

(°C), wind speed (m/s), wind direction, and relative humidity (%). Data were collected every four minutes from 6:00 AM to 7:52 PM on January 1<sup>st</sup>, May 1<sup>st</sup>, July 1<sup>st</sup>, and October 1<sup>st</sup>, corresponding to the Winter, Spring, Summer, and Fall seasons.

Figures 4, 5, 6, and 7 present the measured data, including wind speed (m/s), relative humidity (%), average solar irradiance (W/m<sup>2</sup>), and module irradiance (W/m<sup>2</sup>), both at a 30° tilt, along with average ambient temperature (°C) and module temperature (°C) over the examined days in 2016.



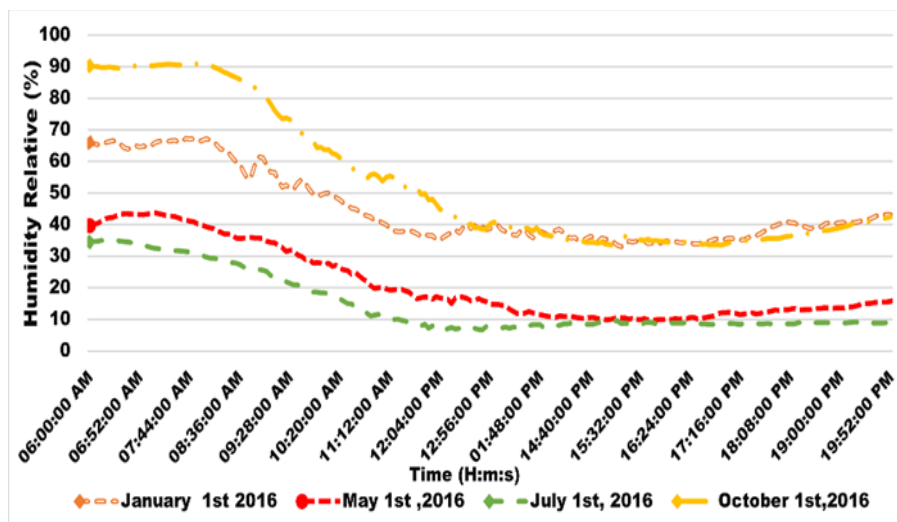
**Fig. 4. Experimental Data of Wind Speed ( $W/m^2$ ) over Four Measured Days in 2016.**

Fig. 4. Displays wind speed data from 6:00 AM to 7:52 PM over four days, each representing a different season, measured by an anemometer.

On January 1<sup>st</sup>, the wind speed starts at 0.02 m/s at 6:00 AM and peaks at 2.56 m/s by 18:32 PM. On May 1<sup>st</sup>, it reaches 8.37 m/s around 6:04 AM and 9:16 AM, then decreases to 4.16m/s by 19:48 PM. On July 1<sup>st</sup>, the wind rises from 7.22 m/s at 6:00 AM to 9.05 m/s at 7:24 AM, then drops to 1.03 m/s by

18:08 PM. On October 1<sup>st</sup>, the wind peaks at 7.20 m/s around noon, decreasing to 2.67 m/s by 19:48 PM.

Wind speed fluctuations are influenced by temperature variations, with stronger winds in summer due to intense heat from the Sahara Desert, as observed on July 1<sup>st</sup>, and weaker winds in winter caused by reduced pressure gradients, as seen on January 1<sup>st</sup>.



**Fig. 5. Experimental Data of Relative Humidity (%) over Four Measured Days in 2016.**

Fig. 5. Presents relative humidity data collected from 6:00 AM to 19:52 PM over four days, with each curve representing seasonal measurements recorded by a thermo-hygrometer.

The data indicate a daily cycle of relative humidity, with higher levels in the early morning and evening,

decreasing during the day. On October 1<sup>st</sup>, humidity peaked at 90% at 6:00 AM and fell to 42% by 19:52 PM. Similarly, on January 1<sup>st</sup>, it started at 67% and dropped to 45%. On May 1<sup>st</sup>, humidity was 42% at 6:00 AM and decreased to 17% by 19:52 PM, while on July 1<sup>st</sup>, it began at 35% and ended at 10%.

The notable daily temperature variations in the OUED-NECHOU region are responsible for fluctuations in humidity levels (Figure 7). As temperatures drop significantly in the early morning and at night, a transient increase in relative humidity occurs. Conversely, intense heating throughout the day leads to very low relative humidity. This daily temperature cycle and the relative humidity (RH) data exhibit an inverse relationship: as temperature rises, RH falls, and vice versa.

In the OUED-NECHOU region, Figures 4 and 5 clearly demonstrate a striking inverse correlation

between relative humidity (%) and wind speed (m/s). Notably, high wind speeds coincide with low humidity during spring and summer (May 1<sup>st</sup> and July 1<sup>st</sup>), while low wind speeds align with high humidity in winter and fall (January 1<sup>st</sup> and October 1<sup>st</sup>). This compelling data underscores the direct relationship between wind speed and relative humidity, revealing that as wind speed increases, relative humidity decreases, and vice versa.

#### IV.2. Measurement Data Analysis of Solar Radiation at 30° Tilt and Temperature (°C).

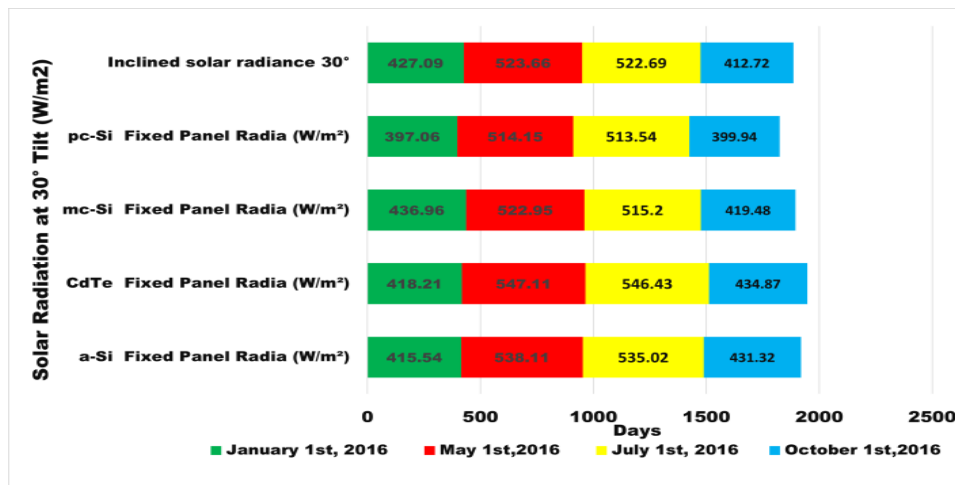


Fig. 6. Experimental Solar Radiation Data at a 30° Inclination (W/m<sup>2</sup>) Over Four Days in 2016 .

Fig.6. Illustrates an experimental comparison of daily average inclined solar irradiance (W/m<sup>2</sup>), measured by a pyranometer, with models solar irradiance (W/m<sup>2</sup>), obtained from calibrated cells, over four days representing different seasons.

The average inclined solar irradiance observed during the experimental days fluctuated in accordance with seasonal weather changes

On January 1<sup>st</sup>, the mc-Si technology exhibited the highest solar irradiance at 436.96 W/m<sup>2</sup>, while the pc-Si technology recorded the lowest value of 397.06 W/m<sup>2</sup>. On May 1<sup>st</sup>, the CdTe and a-Si technologies achieved maximum solar irradiance values of 547.11 W/m<sup>2</sup> and 538.11 W/m<sup>2</sup>, respectively, whereas pc-Si technology recorded a minimum of 514.15 W/m<sup>2</sup>.

On July 1<sup>st</sup>, during summer, the CdTe and a-Si technologies recorded the highest solar irradiance values at 546.43 W/m<sup>2</sup> and 535.02 W/m<sup>2</sup>, respectively, surpassing mc-Si and pc-Si technologies, which measured 515.20 W/m<sup>2</sup> and 513.54 W/m<sup>2</sup>. On October 1<sup>st</sup>, the CdTe and a-Si technologies recorded 434.87 W/m<sup>2</sup> and 431.32 W/m<sup>2</sup>, while the mc-Si and pc-Si technologies measured 419.48 W/m<sup>2</sup> and 399.94 W/m<sup>2</sup>.

Our study found a strong correlation between increased ambient solar irradiance and higher irradiance levels on photovoltaic panels. This highlights the crucial role of ambient irradiance in enhancing solar panel efficiency and demonstrates the significant potential for harnessing solar energy.

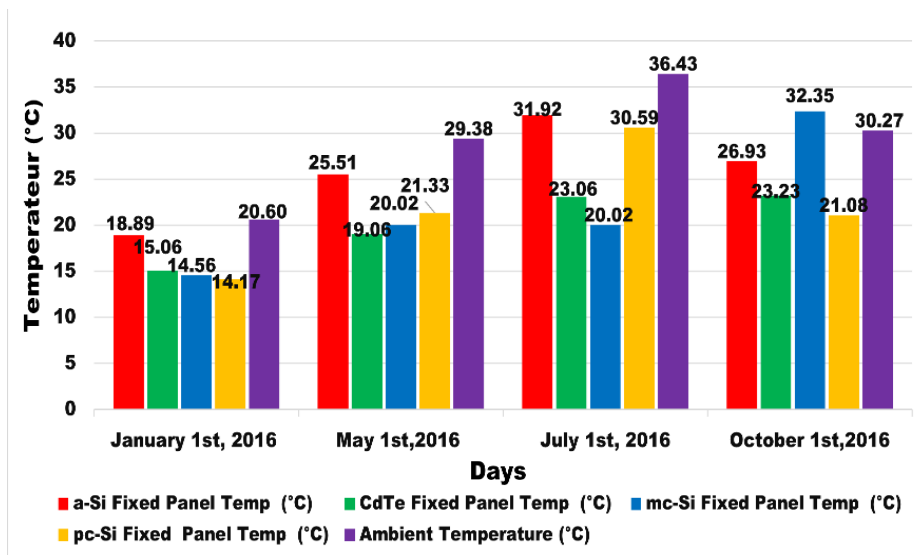


Fig. 7. Experimental data of Ambient temperature °C Over Four Days in 2016.

Fig.7. Comparison of Average Ambient Temperatures Recorded by a Thermo-Hygrometer and Average Temperatures of Fixed Photovoltaic Modules Measured by Cell Sensors Over Four Days.

Temperature data varied by season, with the highest ambient temperature recorded on July 1<sup>st</sup> at 36.43°C (summer), followed by 30.27°C on October 1<sup>st</sup> (fall) and 29.38°C on May 1<sup>st</sup> (spring). The lowest temperature of 20.60°C was observed on January 1<sup>st</sup> (winter), consistent with expected seasonal weather patterns.

The study found that a-Si model consistently exhibited higher surface temperatures compared to other technologies. The highest temperature for a-Si was 31.92 °C on July 1<sup>st</sup>, while the lowest was 18.89 °C on January 1<sup>st</sup>. CdTe models recorded a peak of 23.23 °C on October 1<sup>st</sup> and a low of 15.06 °C on January 1<sup>st</sup>. The mc-Si model peak reached 32.35 °C on October 1<sup>st</sup>, with a minimum of 14.56 °C on January 1<sup>st</sup>, while the pc-Si model showed a high of 30.59 °C on July 1<sup>st</sup> and a low of 14.17 °C on January 1<sup>st</sup>.

Solar irradiance has a direct impact on the temperature of photovoltaic (PV) modules; higher irradiance results in increased energy absorption and elevated module temperatures. This effect is often associated with higher ambient temperatures, especially on sunny days. Observations on May 1<sup>st</sup>, July 1<sup>st</sup>, and October 1<sup>st</sup> confirmed that increased irradiance raised module temperatures, while lower irradiance on January 1<sup>st</sup> led to a temperature decrease.

## V. Performance Analysis

The comparison of solar panel technologies in terms of energy productivity [4],[8]. Or energy grid-injection [9],[10],[06]. Was the topic of many earlier studies; whether in scientific research laboratories or photovoltaic power plants stations, [11],[12],[13]. The performance of a grid-connected PV installation can be evaluated using various characteristics of the solar PV system. These parameters include the final yield (Y<sub>i</sub>), array yield (Y<sub>a</sub>), reference yield (Y<sub>r</sub>), performance ratio (PR), and the total energy generated from the PV system [14],[15],[8]. Assessment can be based on the experimental maximum output power or average output power throughout a year or specific days corresponding to each season.

Evaluating solar panel performance through output power analysis, a key electrical parameter, is crucial for comparative research, particularly when accounting for the specific meteorological conditions of a location. El Mehdi Karami et al. (2018) [16]. Conducted further research to compare the performance of various solar panel technologies. Their study involved measuring the DC power from the modules and the AC power from the inverters using real-time data collected under different weather conditions, including clear, cloudy, and rainy days. Furthermore, another prior studies utilized the concept of comparing maximum output power (kW) across three stationary photovoltaic technologies [8].

This research section presents a comparative performance study of four stationary photovoltaic

subfields, each with an identical capacity of 100 kW, installed at the PV center to evaluate the effectiveness of different PV technologies under the region's climate conditions. Each subfield is oriented to face south and positioned at a 30° tilt angle, which closely matches the region's optimal angle for maximizing solar energy absorption, to capture seasonal variations in system performance. The analysis focuses on three critical aspects: (I) Output Power (including peak power and total power production from sunrise to sunset) and (II) Environmental Factors Influencing Performance, (III) Augmentation Percentage (power output

increase relative to baseline performance). We conducted our experiment by collecting data every 4 minutes from 06:00 AM to 19:52 PM, ensuring thorough monitoring and accurate results. Across the four testing days, the mornings averaged 6 hours and 50 minutes of sunshine, while the evenings provided 6 hours and 36 minutes. Each testing day represented one of the four seasons in 2016: January 1<sup>st</sup> (Winter), May 1<sup>st</sup> (Spring), July 1<sup>st</sup> (Summer), and October 1<sup>st</sup> (Fall). The results of the output power data for each of the four subfields in this study are presented in Figures 8, 9, 10, and 11.

### V.1- Comparative Analysis of Peak Power Output (KW)

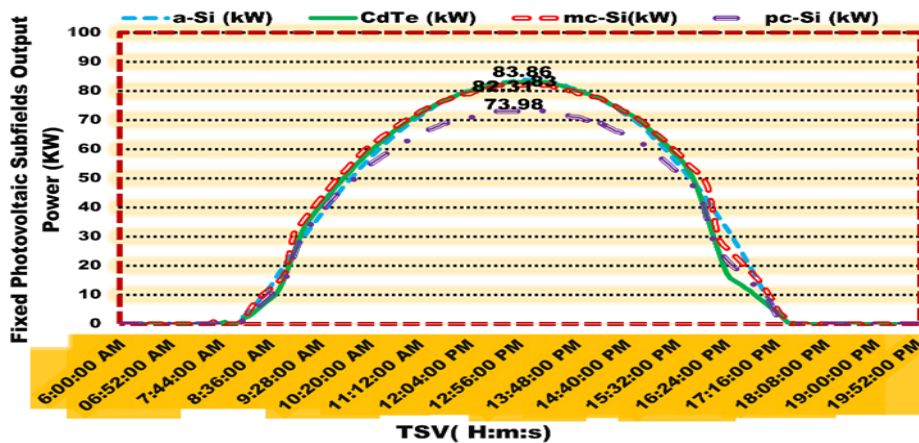


Fig. 8. Power Output Analysis of Four Fixed PV Subfields at a 30° tilt on January 1<sup>st</sup>, 2016, a Winter Day.

Fig. 8. Presents the power output of the a-Si, CdTe, mc-Si, and pc-Si subfields on January 1<sup>st</sup>, 2016. Initially, the output of all four PV technologies was similar. However, by 13:00 PM, differences

became evident, with the mc-Si subfield achieving the highest output at 83.86 kW, followed by a-Si at 83 kW, CdTe at 82.31 kW, and pc-Si at 73.98 kW

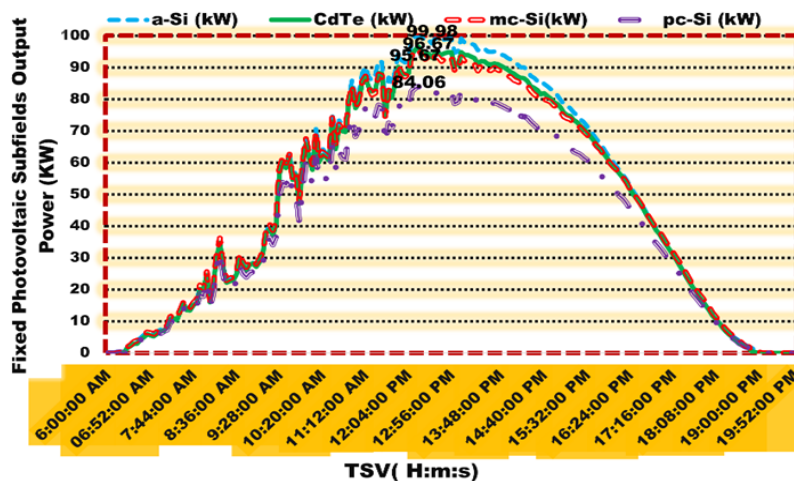


Fig. 9. Power Output Analysis of Four Fixed PV Subfields at a 30° tilt on May 1<sup>st</sup>, 2016, a Spring Day.

The results from the four photovoltaic (PV) subfields on May 1<sup>st</sup>, 2016, are shown in Fig 9 . Highlighting the highest power outputs recorded during the experiment. From 6:00 AM to noon (12:00 PM), the a-Si, CdTe, and mc-Si technologies demonstrated similar performance levels, as

indicated in Figure 11. Specifically, the a-Si subfield achieved the highest output at 99.98 kW, nearing its optimal capacity of 100 kW. The CdTe and mc-Si subfields followed closely, with outputs of 96.67 kW and 95.67 kW, respectively. In contrast, the pc-Si subfield had the lowest output at 84.06 kW.

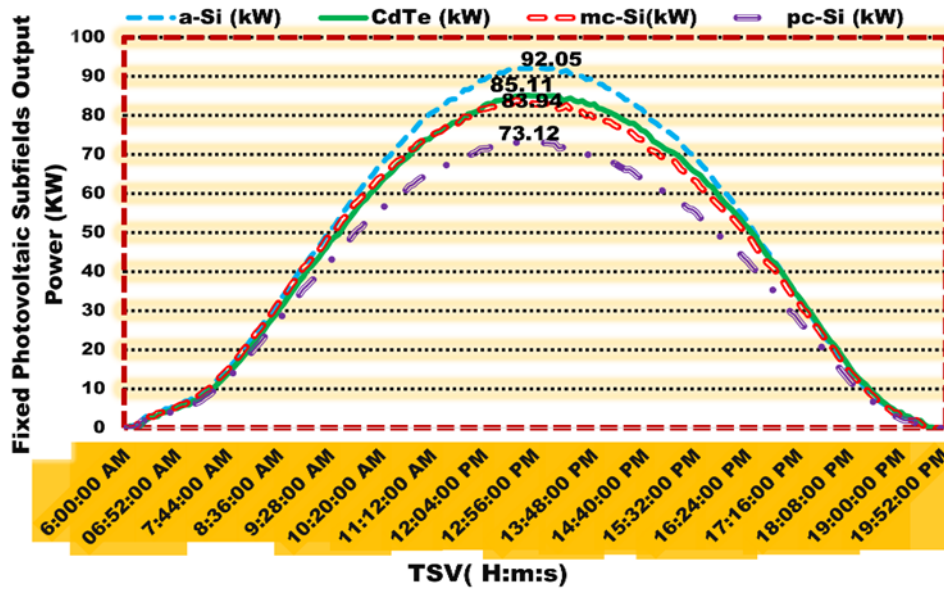


Fig. 10. Power Output Analysis of Four Fixed PV Subfields at a 30° tilt on July 1<sup>st</sup>, 2016, a Summer Day.

The findings from the experimental comparisons of the power output of the four technologies on July 1<sup>st</sup>, 2016, a summer day, are shown in Fig 10. The a-Si subfield continues to demonstrate favorable outcomes, achieving the highest output power of

92.05 kW. Following closely, the CdTe subfield produced 85.11 kW, while the mc-Si subfield recorded an output of 83.84 kW. In contrast, the pc-Si subfield generated the lowest output power at 73.12 Kw.

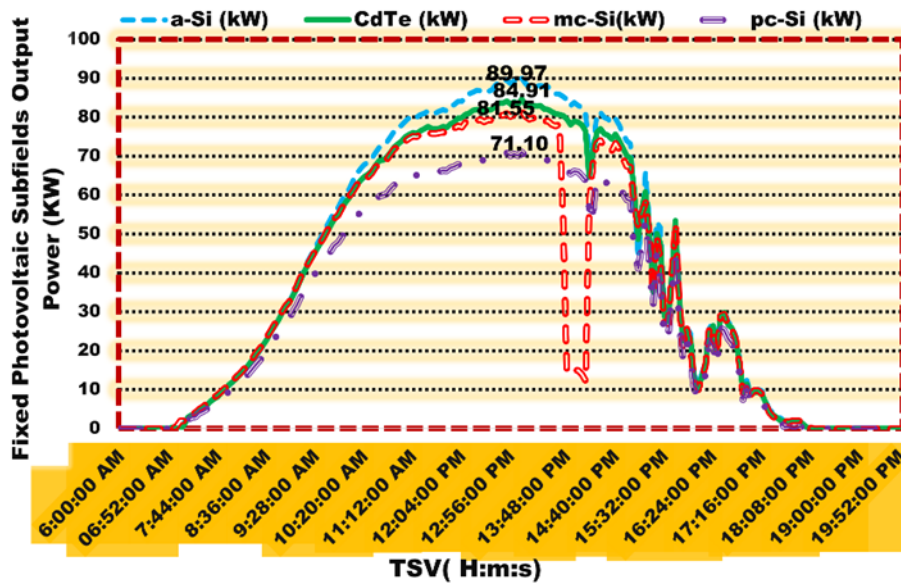


Fig. 11. Power Output Analysis of Four Fixed PV Subfields at a 30° tilt on October 1<sup>st</sup>, 2016, a fall Day.

Fig .11. Experimental Real Data on Output Power for Four Fixed Subfields (a-Si, CdTe, mc-Si, and pc-Si) from October 1<sup>st</sup>. A full-day analysis shows that the a-Si subfield achieved the highest power output at 89.97 kW, followed by the CdTe subfield with 84.91 kW. Additionally, the mc-Si subfield produced 81.55 kW, while the maximum power value of the pc-Si subfield was 71.10 kW, which was lower than that of the other subfields.

Amorphous silicon (a-Si) subfield consistently outperformed other solar technologies across the four experimental days. This finding suggests that amorphous silicon remains a highly effective option for power generation, even with variations in temperature and solar radiation levels throughout the seasons. Therefore, during our study, amorphous silicon technology was reaffirmed as the optimal choice for photovoltaic power generation .

### V.2. The Impact of Meteorological Conditions on Daily Power Output (KW) of Photovoltaic Subfields.

This groundbreaking research underscores the crucial influence of wind speed , humidity, solar irradiance, and module temperature on optimizing the performance of photovoltaic subfields [17],[18]. The data unequivocally demonstrates that heightened wind speeds and decreased humidity levels on May 1<sup>st</sup> and July 1<sup>st</sup> significantly bolstered power output, while elevated humidity on January 1<sup>st</sup> and October 1<sup>st</sup> detrimentally affected efficiency. Moreover, amplified solar irradiance was directly linked to enhanced power generation [19]. Triumphant over potential output reductions caused by escalating cell temperatures. Notably, amorphous silicon (a-Si) subfields exhibited remarkable resistance to temperature surges, maintaining exceptional productivity amidst fluctuating environmental conditions. These findings

undeniably underscore the pivotal importance of favorable climatic factors in realizing optimal solar panel efficiency.

### VI. Augmentation Percentage

Augmentation percentage in renewable energy systems, such as photovoltaic (PV) systems, refers to the improvement in performance or output achieved through various methods or technologies. It quantifies the increase in power, energy production, and efficiency compared to a baseline or reference condition [20] .

Baseline Technology refers to the standard photovoltaic (PV) technology or system used as a reference point for comparison. It represents the most commonly implemented or widely accepted technology in the study and serves as a basis for evaluating alternative configurations or advancements.

This analysis employs the augmentation percentage, derived from daily average output power (kW), to compare four fixed photovoltaic technologies (a-Si, CdTe, mc-Si, and pc-Si) in terms of power gain (kW) on January 1<sup>st</sup> , May 1<sup>st</sup> , July 1<sup>st</sup> , and October 1<sup>st</sup> in 2016. Experimental data was obtained in real time at a frequency of 4 minutes. 2016 . The outcomes of this study are illustrated in the accompanying figures below.

The percentage of augmentation is calculated using the following formula:

$$AP(\%) = \frac{P_{baseline} - P_{new}}{P_{baseline}} \times 100 \quad (1)$$

AP (%): Augmentation Percentage

P<sub>new</sub> : Power output of the new technology or subfield

P<sub>baseline</sub>: Power output of the baseline (reference) technology or subfield.

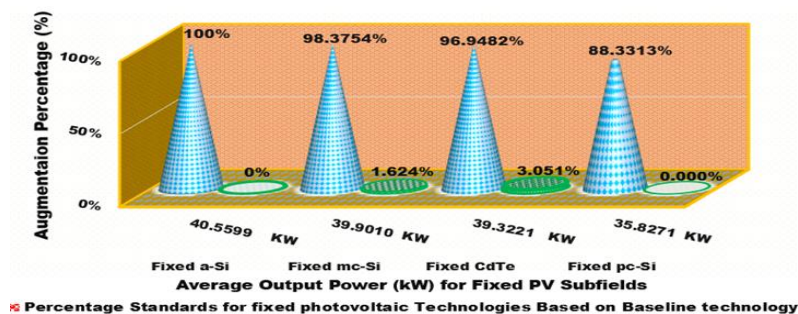


Fig. 12. Percentage Increase in Mean Output Power of Four Fixed PV Subfields on January 1<sup>st</sup> , 2016 (Winter Day).

Data from January 1<sup>st</sup>, 2016, is shown in Fig.12. The average daily power output from the subfields significantly increased due to favourable environmental conditions, including solar radiation and temperature. The mc-Si subfield served as the

power output baseline, showing a 1.624% increase over the a-Si subfield, a 3.051% increase over the CdTe subfield, and an impressive 11.668% gain compared to the pc-Si subfield.

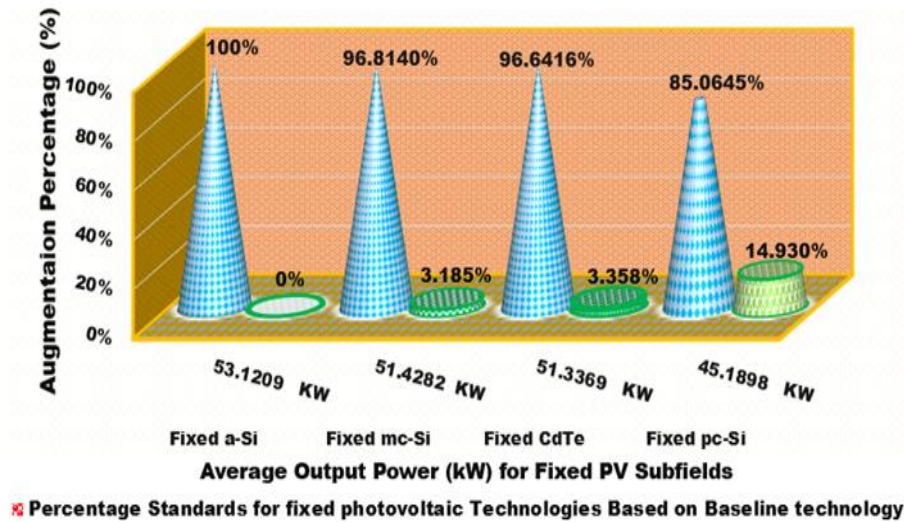


Fig. 13. Percentage Increase in Mean Output Power of Four Fixed PV Subfields on May 1<sup>st</sup>, 2016 (Spring Day).

In Fig. 13, the results from May 1<sup>st</sup>, 2016, show that the a-Si subfield achieved the highest average output power, demonstrating a 3.185% gain over the mc-Si subfield, a 3.385% increase compared to the CdTe

subfield, and a substantial 14.930% boost relative to the pc-Si subfield. These results highlight the exceptional performance of the a-Si subfield under the specific environmental conditions of that day.

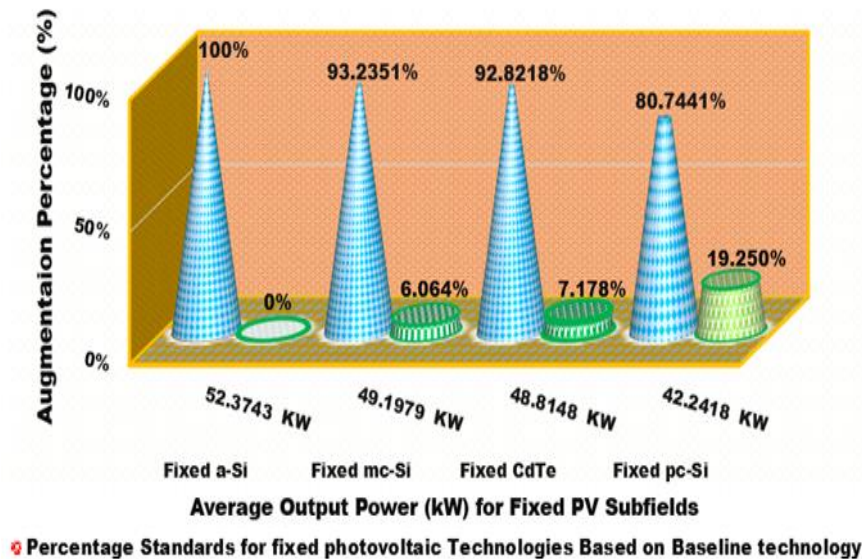
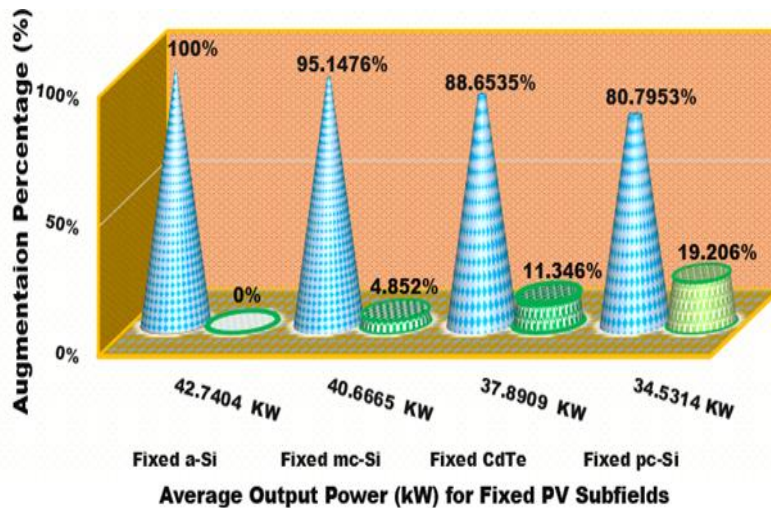


Fig.14. Percentage Increase in Mean Output Power of Four Fixed PV Subfields on July 1<sup>st</sup>, 2016 (Summer Day)

Fig. 14. On July 1<sup>st</sup>, 2016, the a-Si subfield maintained its status as the baseline for power output, showing a 6.064% increase compared to the CdTe subfield and a 7.178% gain relative to the mc-Si subfield. It also achieved a significant 19.250%

increase in power output compared to the pc-Si subfield. These results highlight the a-Si subfield's substantial performance enhancement relative to other experimental days.



Percentage Standards for fixed photovoltaic Technologies Based on Baseline technology

**Fig 15. Percentage Increase in Mean Output Power of Four Fixed PV Subfields on October 1<sup>st</sup>, 2016 (Fall Day).**

On October 1<sup>st</sup>, 2016, on a fall day, Figure 15, following the validation of average output power, the a-Si subfield exhibited a 4.852% increase in power output compared to the CdTe subfield and an 11.346% gain over the mc-Si subfield. Additionally, it achieved a remarkable 19.206% increase compared to the pc-Si subfield, marking one of the highest power gains recorded during the study.

The augmentation percentages were analyzed across four experimental days, focusing on the average output power of four fixed photovoltaic subfields. Power gains varied due to meteorological conditions, including solar irradiance, ambient temperature, wind speed, and relative humidity, which influenced the performance of the technologies subfields. Notably, all PV technologies generated substantial power, with the amorphous silicon (a-Si) subfield achieving optimal output on May 1<sup>st</sup>. Throughout the experimental period, the a-Si subfield consistently outperformed the others, showing significant power gains, particularly on May 1<sup>st</sup>, July 1<sup>st</sup>, and October 1<sup>st</sup>.

## VII. Conclusion

This research paper presents an experimental performance comparison of four fixed photovoltaic (PV) subfields amorphous silicon (a-Si), cadmium telluride (CdTe), monocrystalline silicon (mc-Si), and polycrystalline silicon (pc-Si) each with a capacity of 100 kWp and installed at a 30° tilt angle. The study was conducted on four specific dates in 2016 January 1<sup>st</sup>, May 1<sup>st</sup>, July 1<sup>st</sup>, and October 1<sup>st</sup> representing the four seasons (Winter, Spring, Summer, and Fall), under varying weather

conditions.

Meteorological factors such as wind speed, humidity, solar irradiance, ambient temperature, and module temperature play a crucial role in the performance of photovoltaic (PV) technologies. Our study revealed that higher wind speeds and lower humidity levels on May 1<sup>st</sup> and July 1<sup>st</sup> resulted in increased power output, while the opposite conditions on January 1<sup>st</sup> and October 1<sup>st</sup> led to reduced performance. Increased global solar irradiance also positively affected power output during the same months. However, higher module temperatures decreased output power due to significant drops in output voltage. Throughout the experiments, module temperatures were close to the Standard Test Conditions (STC) of 25°C, which is optimal for power generation. Notably, the amorphous silicon (a-Si) subfields consistently outperformed other technologies, maintaining stable performance even at elevated temperatures due to their lower temperature coefficient, which reduces sensitivity to heat. Furthermore, higher humidity levels on January 1<sup>st</sup> and October 1<sup>st</sup> favored a-Si, enabling it to excel despite lower solar irradiance during those periods.

Based on the maximum output power recorded over the four experimental days in 2016, several key findings emerged. The amorphous silicon (a-Si) subfield achieved the highest power output, reaching 99.98 kW on May 1<sup>st</sup>. On January 8<sup>th</sup>, the polycrystalline silicon (pc-Si) subfield closely followed with a power output of 99.67 kW, while the monocrystalline silicon (mc-Si) subfield reached

99.52 kW on the same day. Additionally, on September 29<sup>th</sup>, the cadmium telluride (CdTe) subfield recorded a power output of 99.17 kW. Notably, the a-Si subfield consistently produced the highest peak DC output power on each experimental day compared to all other subfields.

On May 1<sup>st</sup>, the analysis of the daily average output power showcased the impressive performance of the solar subfields. The amorphous silicon (a-Si) subfield outperformed the others, achieving the highest average output power of 53.1209 kW. Following closely, the monocrystalline silicon (mc-Si) subfield generated 51.4285 kW, while cadmium telluride (CdTe) and polycrystalline silicon (pc-Si) subfields produced 51.3369 kW and 45.1898 kW, respectively.

To enhance the accuracy of this experimental study, an augmentation percentage factor was adopted to analyze the increase and gain in power. The amorphous silicon (a-Si) technology served as the baseline on May 1<sup>st</sup>, July 1<sup>st</sup>, and October 1<sup>st</sup>, demonstrating higher power gains on nearly all experimental days. The highest production was recorded on July 1<sup>st</sup> and October 1<sup>st</sup>, with power gains of 6.064% over the cadmium telluride (CdTe) subfield, 7.178% more power than the monocrystalline silicon (mc-Si) subfield, and 19.250% more power than the polycrystalline silicon (pc-Si) subfield on July 1<sup>st</sup>. Conversely, the mc-Si subfield served as the baseline on January 1<sup>st</sup>, achieving the highest power gain of 11.668% compared to the pc-Si subfield.

Our future research aims to conduct an experimental comparative analysis of fixed and single-axis tracking photovoltaic subfields installed at the OUED-NECHOU Solar Photovoltaic Power Panels Center. The study will focus on power productivity, power increase, and the influence of meteorological conditions on performance. And prove the significant role of tracking systems in solar panels in enhancing the productivity and capturing a tremendous amount of solar radiation.

### Acknowledgment

The authors sincerely appreciate the unwavering support of the solar power plants pilot center team at Oued-Nechou, Ghardaïa, for their invaluable assistance in our research.

### I. References

[1] GK. Singh, "Solar power generation by PV (photovoltaic) technology: A review," *Energ*, vol.

53, pp. 1–13, 2013.

[2] AJ. Carr, TL. Pryor, "A comparison of the performance of different PV module types in temperate climates," *Sola . Energ*, vol. 76, pp. 285–294, 2004.

[3] J.A. del Cueto, "Comparison of energy production and performance from flat-plate photovoltaic module technologies deployed at fixed tilt," *IEEE Photovol .Speciali. Confer*, pp. 1523–1526, 2002 [Conf Record of the Twenty-Ninth].

[4] C. Cañete, J. Carretero, de-CM. Sidrach, "Energy performance of different photovoltaic module technologies under outdoor conditions," *Energ*, vol. 65, pp. 295-302, February 2014.

[5] S. Edalati, M. Ameri b, M. Iranmanesh, "Comparative performance investigation of mono- and poly-crystalline silicon photovoltaic modules for use in grid-connected photovoltaic systems in dry climates," *Appli Energ*, vol. 160, pp. 255–265, 2015.

[6] A. Attari, A. EL yaakoubi, A. Asselman, "Comparative Performance Investigation Between Photovoltaic Systems from two Different Cities," *Proce .Engineer*, vol. 181, pp. 810 – 817, 2017 [10th internati conf interdisciplinary in Engineering]

[7] Y M. Effendy, H. Hashim, K. Tamer, M R M. Amran, "A comparative study of three types of grid connected photovoltaic systems based on actual performance," *Energ Convers*, vol. 78, pp. 8–13, February 2014.

[8] A. Ameer, A. Sekkat, S. Loudiyi, M. Aggour, "Performance evaluation of different photovoltaic technologies in the region of Ifrane, Morocco," *Energ for Sustaina Develop*. vol. 52, pp. 96–10, 2019.

[9] L. BOUHAKI, R. SAADANI, R. AGOUNOUN, K. SBAI, M. RAHMOUNE, "Simulation et comparaison des trois technologies des modules photovoltaïques raccordés au réseau," 13<sup>ème</sup> Congrès de Mécanique, Meknès, MAROC, pp. 11–14, Avril 2017.

[10] L M. Ayompe, A. Duffy, S J. McCormack, N. Sneddon, "Measured performance of a 1.72 kW rooftop grid connected photovoltaic system in Ireland," *Energ convers manage*, vol. 52, pp. 816–825, 2011.

[11] A. Elamim, B. Hartiti, A. Haibaou, A. Lfakir, P. Thevenin, "Analysis and comparison of different

PV technologies for determining the optimal PV panels- A case study in Mohammedia , Morocco,” *Journ of Electron and Electron Engineer*, vol. 12, pp. 37–45, 2017.

[12] B. Marion, J. Adelstein, K. Boyle, H. Hayden, B. Hammond, T. Fletcher, B. Canada, D. Narang, A. Kimber , L. Mitchell , T. Townsend, “Performance Parameters for Grid-Connected PV Systems,” *Conference Record of the Thirty-first IEEE Photovoltaic Specialists Conference*, Lake Buena Vista, FL, USA , pp. 1601–1606, January 2005.

[13] J. Lelouxa , L. Narvartea, D. Treboscb, “Review of the performance of residential PV systems in France,” *Renewa and Sustaina Energ Revie*, vol. 16, pp. 1369–1376, 2012.

[14] A. Al-Otaibi, A. Al-Qattan, F. Fairouz, A. Al-Mulla, “Performance evaluation of photovoltaic systems on Kuwaiti schools,” *Energ Convers and Manage*, vol. 95, pp. 110–119, 2015.

[15] PM. Congedo, M. Malvoni, M G. De Giorg , “Performance measurements of monocrystalline silicon PV modules in South-eastern Italy,” *Energ Convers and Manage*, vol. 68, pp. 1–10, April 2013.

[16] E. KARAMI, M. RAFI, A. RIDAH, H. Bouchaib, P. Thevenin, “Analysis of measured and simulated performance data of different PV modules of silicon in Casablanca,” *the seco. internati. conf. on smar. applicat. and data analy. for smar. sites* , February 2018.

[17] C. Bahanni, M. Adar, S. Boulmrharj, M. Khaidar, M. Mabrouki, “Performance comparison and impact of weather conditions on different photovoltaic modules in two different cities,” *Indones Jour of Electri Engineer and Compr Scien* , vol. 25, pp. 1275–1286, March 2022.

[18] Q. Xia, “Study on The Relationship Between Meteorological Factors and Photovoltaic Power Generation Efficiency and Influence Mechanism ,” *Conf. Series: Earth and Environmental Science*, vol. 769, 2021.

[19] Al. Adnan, M. Al-Dweri, A. Al-Ghandoor, B. Hammad, W. Al-Kouz, “Analysis of Effects of Solar Irradiance, Cell Temperature and Wind Speed on Photovoltaic Systems Performance,” *Internat. Jour. of Energ Econom and Polic London*, vol. 10, pp. 353-359, October 2019.

[20] L. Abu Hussein, O. Ayadi, M. Fathi, “Performance Comparison for Sun- Tracking

Mechanism Photovoltaic (PV) and Concentrated Photovoltaic (CPV) Solar Panels with Fixed System PV Panels in Jordan” *IEEE 12th Internati. Renew. Engineeri. Conf*, pp. 1-8, April 2021.